Redox Biology 64 (2023) 102779

Contents lists available at ScienceDirect

Redox Biology

journal homepage: www.elsevier.com/locate/redox

Apolipoprotein E is required for brain iron homeostasis in mice

Juan Ma [a,c], Qian Guo [b,d,**], Meng-Qi Shen [a], Wei Li [a], Qi-Xin Zhong [e], Zhong-Ming Qian [a,*]

[a] Department of Neurology, Affiliated Hospital, and Institute of Translational and Precision Medicine, Nantong University, 19 Qi Xiu Road, Nantong, Jiangsu, 226001, China
[b] Institute of Geriatrics (Shanghai University), Affiliated Nantong Hospital of Shanghai University (The Sixth People's Hospital of Nantong), School of Medicine, Shanghai University, 881 Yonghe Road, Nantong, Jiangsu, 226001, China
[c] Laboratory of Neuropharmacology of Pharmacy School, and National Clinical Research Center for Aging and Medicine of Huashan Hospital, Fudan University, Shanghai, 201203, China
[d] Shanghai Engineering Research Center of Organ Repair, School of Medicine, Shanghai University, 99 Shangda Road, Shanghai, 200444, China
[e] Department of Cardiovascular Medicine, Shenzhen Hospital, Guangzhou University of Chinese Medicine, Shenzhen, 518034, China

ARTICLE INFO

Keywords:
Apolipoprotein E knock-out (ApoE KO/ApoE$^{-/-}$) mice
Brain iron metabolism
TfR1 and Fpn1
IRPs and hepcidin
AD and amyloid beta
Reactive oxygen species (ROS)
Cytokines
Glutathione peroxidase 4 (Gpx4)

ABSTRACT

Background: Apolipoprotein E deficiency (ApoE$^{-/-}$) increases progressively iron in the liver, spleen and aortic tissues with age in mice. However, it is unknown whether ApoE affects brain iron.
Methods: We investigated iron contents, expression of transferrin receptor 1 (TfR1), ferroportin 1 (Fpn1), iron regulatory proteins (IRPs), aconitase, hepcidin, Aβ42, MAP2, reactive oxygen species (ROS), cytokines and glutathione peroxidase 4 (Gpx4) in the brain of ApoE$^{-/-}$ mice.
Results: We demonstrated that ApoE$^{-/-}$ induced a significant increase in iron, TfR1 and IRPs and a reduction in Fpn1, aconitase and hepcidin in the hippocampus and basal ganglia. We also showed that replenishment of ApoE absent partly reversed the iron-related phenotype in ApoE$^{-/-}$ mice at 24-months old. In addition, ApoE$^{-/-}$ induced a significant increase in Aβ42, MDA, 8-isoprostane, IL-1β, IL-6, and TNFα and a reduction in MAP2 and Gpx4 in hippocampus, basal ganglia and/or cortex of mice at 24-months old.
Conclusions: Our findings implied that ApoE is required for brain iron homeostasis and ApoE$^{-/-}$-induced increase in brain iron is due to the increased IRP/TfR1-mediated cell-iron uptake as well as the reduced IRP/Fpn1 associated cell-iron export and suggested that ApoE$^{-/-}$ induced neuronal injury resulted mainly from the increased iron and subsequently ROS, inflammation and ferroptosis.

1. Introduction

Iron is a key participator and regulator of physiological activities in the brain, while excess iron has been associated with formation of free radicals and oxidative damage to neuronal or other brain cells [1]. Abnormally increased iron in the brain has been observed in various neurodegenerative disorders including Alzheimer's disease (AD) [2–6], and a potential role of the increased brain iron in the development of AD has been suggested [6–8]. Many studies have also shown that the increased brain iron, induced by the errors in brain iron metabolism found in neurodegenerative disorders, have a multi-factorial pathogenesis, including genetic and nongenetic (eg, toxic exposure, environmental agents) factors [9,10].

It has been also speculated that Apolipoprotein E (ApoE) may contribute to AD pathogenesis as ApoE is able to bind beta Amyloid (Aβ) and eliminate toxic Aβ peptides out of the brain via ApoE receptors [11]. In humans, there are three structurally different ApoE isoforms, named ApoE2, ApoE3, and ApoE4, which are the products of the ε2, ε3 and ε4 alleles [12]. Peripherally, the majority of ApoE in plasma is derived from hepatocytes [13]. In the brain, ApoE is produced mainly by astrocytes [13]. It has been reported that plasma/serum and brain ApoE levels decrease in AD patients [14,15]. The Alzheimer's risk allele, ApoE4A, up-regulates the levels of iron storage protein ferritin [16] and dose associates with increased brain iron and β-amyloid via blood-brain barrier dysfunction [17]. These findings reveal that elevated brain iron has adverse outcomes on AD progression, and introduce that brain iron elevation is a possible mechanism behind ApoE4 being the major genetic risk factor for AD [16,18,19].

Iron has therefore been considered as a missing link between ApoE

* Corresponding author. Institute of Translational and Precision Medicine, Nantong University, 19 Qi Xiu Road, Nantong, 226001, China.
** Corresponding author. School of Medicine, Shanghai University, 99 Shangda Road, Shanghai, 200444, China.
E-mail addresses: mj19890412@126.com (J. Ma), qian_guo@shu.edu.cn (Q. Guo), MQ0624@163.com (M.-Q. Shen), liweinantong@163.com (W. Li), zhongqixin2022@163.com (Q.-X. Zhong), zhongmingqian2022@163.com (Z.-M. Qian).

https://doi.org/10.1016/j.redox.2023.102779
Received 30 May 2023; Accepted 8 June 2023
Available online 15 June 2023

Abbreviations

Aβ	β-amyloid
AD	Alzheimer disease
ApoE	Apolipoprotein E
$ApoE^{-/-}$	Apolipoprotein E knock-out
CSF	Cerebrospinal fluid
FAC	Ferric ammonium citrate
Fpn1	Ferroportin 1
FTH	Ferritin heavy chain
FTL:	Ferritin light chain
GFAAS	graphite furnace atomic absorption spectrophotometer
Gpx4	Glutathione peroxidase 4
IL-1β	Interleukin-1β
IL-6	Interleukin-6
IL-10	Interleukin-10
IRPs	Iron regulatory proteins
MAP2	Neuron microtubule-associated protein 2
MCI	Mild cognitive impairment
MDA	Malondialdehyde
PBS	Phosphate buffered saline
ROS	Reactive oxygen species
TBA	Thiobarbituric acid
TfR1	Transferrin receptor 1
TNF-α:	Tumor necrosis factor-α
WT	Wild-type

and AD [20]. Up to now, very little is known about whether ApoE has a role in brain iron homeostasis and how ApoE affects brain iron metabolism. Recently, we demonstrated that ApoE deficiency ($ApoE^{-/-}$) could progressively increase iron in the liver, spleen and aortic tissues with age in mice, suggesting the existence of an essential role of ApoE in iron homeostasis [21,22]. However, the effects of ApoE on brain iron homeostasis are unknown. Based on the above findings, we hypothesized that ApoE may also have a role in brain iron homeostasis as it works outside brain.

In the present study, we firstly investigated the effects of $ApoE^{-/-}$ on brain iron status by determining the total iron level and ferritin expression in different brain regions in $ApoE^{-/-}$ and wild-type (WT) mice at different ages. To find out the mechanisms involved in the $ApoE^{-/-}$- induced changes in brain iron status, we secondly dissected the expression of key contributors to cell and tissue iron balance, transferrin receptor 1 (TfR1, the major cell-iron importer) and ferroportin 1 (Fpn1, the iron exporter), and also the major controller of TfR1 and Fpn1 expression, including iron regulatory proteins (IRPs) and hepcidin. Thirdly, we investigated effects of the impact of $ApoE^{-/-}$ on expression of a pathological marker of AD, beta Amyloid1-42 (Aβ42), and also neuron microtubule-associated protein 2 (MAP2), heme oxygenase 1 (HO1), indexes of reactive oxygen species (ROS), malondialdehyde (MDA) and 8-isoprostane, relevant cytokines and glutathione peroxidase 4 (Gpx4) in the brain of mice at 24-months old. To confirm the role of ApoE in brain iron homeostasis, we finally performed rescue experiments by replenishing ApoE in mutant mice. Our findings suggested that ApoE may be required for brain iron homeostasis.

2. Materials and methods

2.1. Materials

Unless otherwise stated, all chemicals including mouse monoclonal anti-β-actin were obtained from the Sigma Chemical Company, St. Louis, MO, USA. Mouse anti-human TfR1, Alexa Fluor 488 goat anti-rabbit IgG, TRIzol reagent, RPMI-1640 medium and fetal bovine serum were purchased from Invitrogen Life Technologies, Carlsbad, CA, USA; rabbit polyclonal anti-mouse Fpn1 from Novus Biologicals, Littleton, CO, USA; rabbit polyclonal anti-FTL (ferritin light chain) from Proteintech, Chicago, IL, USA; rabbit polyclonal anti-FTH (ferritin heavy chain) from Bioworld Technology Inc., Louis Park, MN, USA; rabbit anti-MAP2, rabbit anti-Aβ42, rabbit anti-HO1, rabbit anti-Gpx4, rabbit anti-ApoE, rabbit anti-IRP1 (iron regulatory protein 1) and rabbit anti-IRP2 (iron regulatory protein 2) from Abcam, Cambridge, MA, USA; and goat anti-rabbit or anti-mouse IRDye 800 CW secondary antibody from LI-COR Biosciences, Lincoln, Nebraska, USA. AevertAid First Strand cDNA Synthesis Kit and BCA protein assay kits were bought from Thermo Scientific, Waltham, MA, USA; Faststart Universal SYBR Green Master and LightCycler96 from Roche, Nutley, NJ, USA; and protein RIPA lysis buffer from the Beyotime Institute of Biotechnology, Haimen, JS, China. All solutions were prepared fresh, prior to each assay.

2.2. Animals and treatments

SPF (specific pathogen-free) grade male ApoE-deficient ($ApoE^{-/-}$) and wild-type (WT, age and gender matched) C57-BL/6 mice were purchased from Hua Fu Kang Biotechnology Co., Ltd (Beijing, China) and verified by RT-PCR genotyping as described previously [23]. A total of 53 male mice (n = 20 in WT and n = 25 + 8 in $ApoE^{-/-}$) were used in this study. The mice were respectively killed at 1-, 2-. 4-, 10- and 24-months (All n = 4 in WT and n = 5 in $ApoE^{-/-}$) for all designed measurements. Another 8 $ApoE^{-/-}$ mice at 24-months old were treated with Ad-Blank (n = 4) or Ad-ApoE (n = 4) for rescue experiments (Supplementary Fig. 1). The mice were housed under SPF conditions at 22±2 °C with a relative humidity of 60–65% and maintained under a 12-h light/12-h dark cycle with ad libitum access to food and water as described previously [24,25]. All animal care and experimental protocols were performed according to the Animal Management Rules of the Ministry of Health of China, and approved by the Animal Ethics Committees of Nantong University (NSFC31271132).

2.3. Intracerebroventricular injection

The ApoE-overexpressing adenovirus (Ad-ApoE) and blank virus (Ad-blank) with a titer of 1×10^{11} plaque-forming units [pfu]/μl were constructed by Obio Technology Corp., Ltd. (Shanghai, China). Intracerebroventricular (ICV) injection of Ad-ApoE or Ad-blank was performed as previously described [26]. The mice were anesthetized with 1% pentobarbital sodium (40 mg/kg body weight, i.p.) via i.p. injection and were secured in a stereotaxic instrument. 2 μL ([pfu]/μl) of Ad-ApoE or Ad-blank were injected bilaterally into the lateral ventricle according to a standard stereotaxic atlas (−3.0 mm dorsal/ventral, −1.0 mm lateral, and −0.5 mm anterior/posterior from the bregma) using a 10 μl syringe with a 33 gauge needle at a rate of 0.5 μl/min. The syringe was left in place for an additional 5 min before removal.

2.4. Tissue samples preparation

Animals were anesthetized and decapitated. After perfusion with phosphate-buffered saline (PBS, Milli-Q water prepared and DEPC treated, pH 7.4) through the left ventricle, the brain was rapidly removed, immediately dissected into three brain regions: cortex, hippocampus and basal ganglia for iron content determination, RT-PCR, western blot analysis and other measurements, or fixed in 4% paraformaldehyde, dehydrated in graded ethanol, embedded in paraffin, and cut into 4-μm-thick sections for tunel Assay and immunohistochemistry [27].

2.5. Western blot analysis

Tissue were washed and homogenized as described previously [28]. After centrifugation at 14,000 rpm for 15 min at 4 °C, the supernatant was collected and protein content was determined using the BCA protein Assay kit [29]. Proteins were heated for 10 min at 100 °C in sample buffer (125 mM Tris/HCl, 2% (w/v) SDS, 5% (v/v) 2-mercaptoethanol, 10% (v/v) glycerol, 0.001% (w/v) bromphenol blue, pH 6.8). Aliquots of the extract containing about 30 μg of protein were loaded and run on a single track of 12% SDS-PAGE under reducing conditions and were subsequently transferred to a pure nitrocellulose membrane. The blots were blocked and then incubated with primary antibodies: mouse anti-human TfR1 (1:1000), rabbit polyclonal anti-mouse Fpn1 (1:1000), rabbit polyclonal anti-FTL (1:1000) and anti-FTH (1:1000), rabbit monoclonal anti-IRP1 (1:1000), rabbit monoclonal anti-IRP2 (1:1000), and rabbit anti-MAP2 (1:1000), anti-Aβ42 (1:500) and anti-ApoE (1:1000) overnight at 4 °C. After being washed, the blots were incubated with goat anti-rabbit or anti-mouse IRDye 800 CW secondary antibody (1:5000) for 2-h at 37 °C [30]. The intensity of the specific bands was detected and analyzed by Odyssey infrared image system (Li-Cor, Lincoln, NE, USA).

2.6. Isolation of total RNA and quantitative real-time PCR

Total RNA extraction and cDNA preparation were performed using TRIzol reagent and the AevertAid First Strand cDNA synthesis kit respectively, in accordance with the instructions of the manufacturers. Quantitative real-time PCR was carried out using FastStart Universal SYBR Green Master and LightCycler96. The specific pairs of primers of mouse β-actin, hepcidin, FTL, FTH, interleukin-1β (IL-1β), interleukin-6 (IL-6), interleukin-10 (IL-10), tumor necrosis factor-α (TNFα) and Gpx4 are listed in Supplementary Table 1. The CT value of each target gene was normalized to that of β-actin mRNA. Relative gene expression was calculated by the $2^{-\Delta\Delta CT}$ method [31].

2.7. Measurement of cytosolic aconitase activity

Cytosolic aconitase activity was measured as described previously [32]. The tissues were homogenized in 0.27 M sucrose buffered to pH 7.4 with Hepes and then centrifuged at 10,000g at 4 °C for 15 min. The supernatant obtained was recentrifuged at 35,000g at 4 °C for 30 min and used as "cytosol." The diluted supernatant was added into 20 mM aconitate substrate solution (pH 7.4) containing 0.02% BSA. Cytosolic aconitase activity was determined by the measurement of changes in absorbance of 240 nm at intervals of 15 s at 25 °C for a few minutes. Bovine heart aconitase (purified) was run in parallel to samples and applied to establish standard curve. On the basis of the standard curve, cytosolic aconitase activity was calculated. The results in enzymatic activity were expressed miliunits (mU) per mg of protein".

2.8. GFAAS

The total iron (μg/g wet weight) in the tissues was determined using a graphite furnace atomic absorption spectrophotometer (GFAAS) as previously described [33]. In brief, tissues were homogenized in 20 mM HEPES followed by digestion in equal volume of ultra-pure nitric acid and then were measured with a GFAAS (Perkin-Elmer, Analyst 100). Standard curves were prepared by diluting iron standard with blanks prepared from homogenization reagents in 0.2% HNO_3 [33].

2.9. DAB-enhanced perls' staining

Paraformaldehyde-fixed paraffin-embedded tissues were sectioned into 20 μM sections and stored at room temperature. Slides were the blocked for nonspecific binding using protein block, and endogenous peroxidase activity was quenched [34] For DAB-enhanced Perls staining, slides were immersed for 1-h in 1% potassium ferricyanide in 0.1-M HCl buffer and then stained with DAB chromogen substrate. All slides were counterstained with hematoxylin and then visualized using a Nikon Eclipse TE2000-Umicroscope (Nikon, UK).

2.10. Determination of malondialdehyde and 8-isoprostane

Malondialdehyde (MDA) is an end-product of per-oxidized fatty acid and a marker of lipid peroxidation and free radical activity. It was measured by the thiobarbituric acid (TBA) reaction with a commercial kit. MDA concentrations were calculated by the absorbance of TBA reactive substances (TBARS) at 532 nm using a Beckman DU-68 spectrophotometer [35]. 8-isoprostane was determined using a ELISA Kit (ab175819). Tissues of three brain regions were processed according to the producer's instructions. Each ELISA sample was tested in duplicates according to the manual of 8-isoprostane ELISA Kit. Absorbance readings at 450 nm were normalized to readings of Maximum Binding Control, and quantified into pg/ml using an 8-isoprostane standard curve [36,37].

2.11. TUNEL assay

Terminal deoxynucleotidyl transferase-mediated biotinylated dUTP nick-end labeling (TUNEL) staining was performed b use of in situ cell death detection kit (Roche, 11684817910) according to the manufacturer's instruction. Paraffin-embedded (after deparaffinization in xylenes) tissue sections were washed with PBS and treated with Proteinase K solution by incubating them in a humidity chamber for 30 min at room temperature, then blocking endogenous peroxidase with H_2O_2 for 10 min. After that, slides were incubated with TdT and dUTP (2:29) at 37 °C for 2 h, and then were incubated in converter-POD at room temperature for 30 min. Finally, slides were developed using the Dako Envision HRP-DAB System and stained with hematoxylin for 3 min in turns at room temperature [38]. Tissue sections were visualized using a standard bright field microscope.

2.12. Immunohistochemistry

Formalin-fixed paraffin-embedded tissues were sectioned into 0.5-μm sections and stored at room temperature. Sections were deparaffinized using xylene and rehydrated in ethanol before being subjected to heat-activated antigen retrieval in citrate buffer (pH 6.0). Slides then were blocked for nonspecific binding using protein block, and endogenous peroxidase activity was quenched, stained with primary antibodies: rabbit anti-FTL (1:100), rabbit anti-Aβ42 (1:200) and rabbit anti-MAP2 (1:150), then were developed using the Dako Envision HRP-DAB System. All slides were counterstained with hematoxylin and then were visualized using a standard bright field microscope [39,40].

2.13. Immunofluorescence examination

Immunofluorescence staining was carried out as described [41]. In brief, slices were incubated in blocking solution followed by overnight incubation at 4 °C with primary antibody (rabbit anti-HO1, 1:200). After washing with PBS, the slides were incubated with Alex Fluor 488, conjugated secondary antibodies for 1 h at 37 °C. The nuclei were counterstained with DAPI. The slides with immunofluorescence staining were visualized with a confocal microscope (Carl Zeiss; Heidenheim, Germany).

2.14. The rescue effect of overexpression of ApoE in $ApoE^{-/-}$ mice

To assess the rescue effect of over-expression of ApoE in $ApoE^{-/-}$ mice, 2 μL ([pfu]/μl) Ad-ApoE or Ad-blank was administered to $ApoE^{-/-}$ mice at 24-months old by intracerebroventricular (ICV) injection, and 7 days later the relevant measurements were performed.

2.15. Statistical analysis

Statistical analyses were performed using Graphpad Prism 5 (Graphpad software, La Jolla, CA). Data were presented as mean ± SEM. The differences between the means were all determined by one or two-way analyses of variance (ANOVA). A probability value of $p < 0.05$ was taken to be statistically significant.

3. Results

3.1. ApoE deficiency resulted in a significant increase in iron content in the hippocampus and basal ganglia of mice at 10 and/or 24 months old

To find out whether ApoE affects brain iron homeostasis, we first measured total iron contents in the cortex, hippocampus and basal ganglia of mice of ApoE$^{-/-}$ and WT mice at different age (1-, 2-, 4-, 10- and 24-months old). Although iron contents in the cortex (Fig. 1A) of ApoE$^{-/-}$mice at 4-, 10- and 24-months were higher than those in WT mice, the differences were not significant. However, in the hippocampus at 24-months old (Fig. 1B) and in basal ganglia at 10- and 24-months old (Fig. 1C), iron contents were significantly higher in ApoE$^{-/-}$ than in WT mice. The similar findings were also found in DAB-enhanced Perls' iron staining of cortex (Fig. 1D), hippocampus (Fig. 1E) and basal ganglia (Fig. 1F) of ApoE$^{-/-}$ and WT mice at age of 24-months old; iron content in hippocampus and basal ganglia being also higher in ApoE$^{-/-}$ than in WT mice. Then, we detected expression of H-subunit (FTH) and L-subunit (FTL) of ferritin, the intracellular proteins responsible for the sequestration and storage of iron, in the cortex, hippocampus and basal ganglia of ApoE$^{-/-}$ and WT mice at 24-months old. Western blot analysis showed that both FTL (Fig. 1G and H) and FTH (Fig. 1G and I) protein expression in the hippocampus and basal ganglia was significantly higher in ApoE$^{-/-}$ than that in WT mice. In the cortex, expression FTL (Fig. 1G and H) and FTH (Fig. 1G and I) was also higher in ApoE$^{-/-}$ than that in WT mice, but the differences were not significant. The very similar findings were observed in FTL (Fig. 1J) and FTH (Fig. 1K) mRNA expression which was also significantly higher in the hippocampus and basal ganglia, but not in the cortex of ApoE$^{-/-}$ than that in WT mice. Immunohistochemistry in the cortex (Fig. 1L), hippocampus (Fig. 1M) and basal ganglia (Fig. 1N) revealed the same outcomes as Western blot and RT-PCR analysis.These results implied that ApoE$^{-/-}$ could induce a progressive increase in iron contents with age in these two brain regions and indicated that the effects of ApoE$^{-/-}$ on brain iron contents were

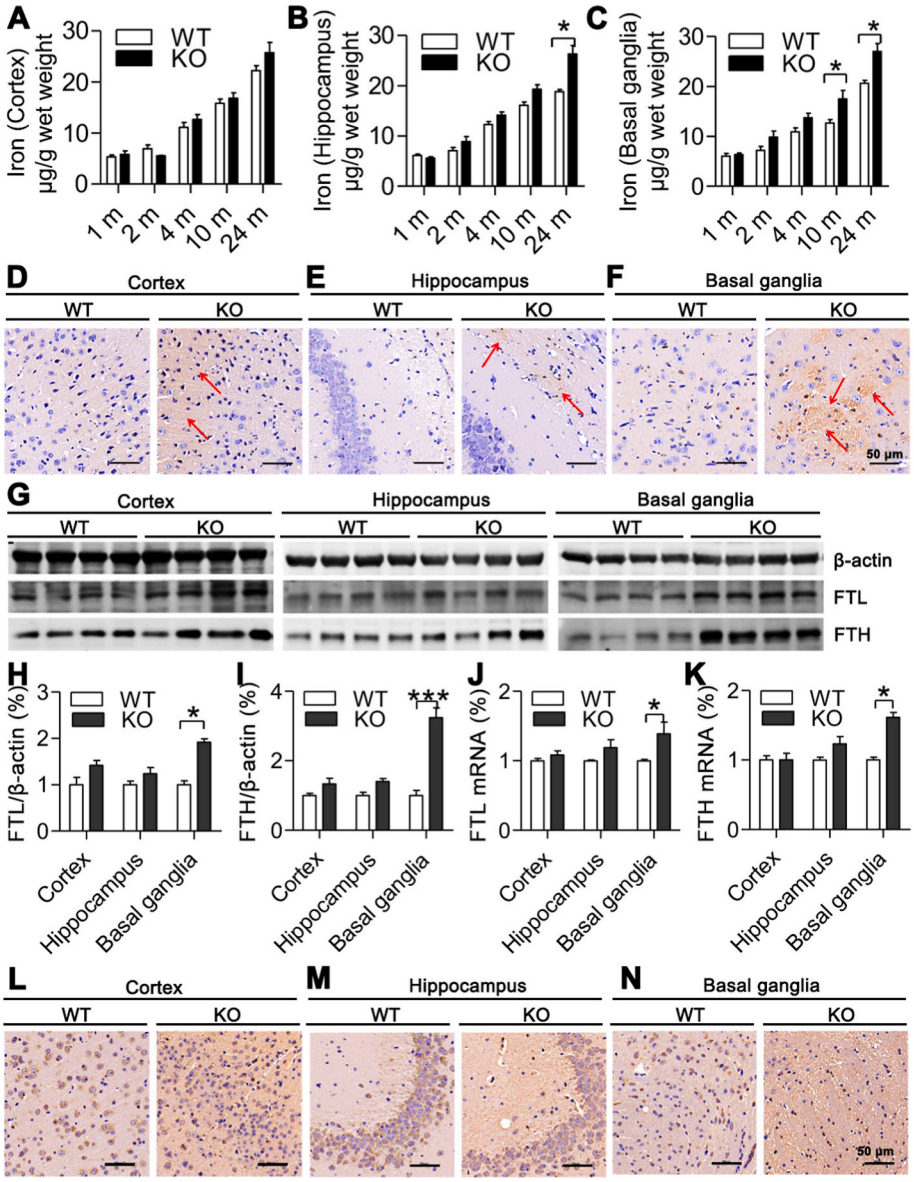

Fig. 1. Effects of ApoE deficiency on iron content and expression of FTL and FTH in the cortex, hippocampus and basal ganglia of mice at different ages or at 24-months old.
A-C. Total iron contents (μg/g ww = wet weight) in the cortex (**A**), hippocampus (**B**) and basal ganglia (**C**) of ApoE$^{-/-}$ (n = 4) and WT (n = 4) mice at 1-, 2-, 4, 10, and 24-months old were measured by a GFAAS; **D-F.** DAB-enhanced Perls' iron staining of cortex, hippocampus and basal ganglia (Scale bar = 50 μm) of ApoE$^{-/-}$ (n = 4) and WT (n = 4) mice at age of 24-months old; **G-I.** Western blot analysis of FTL (**G** and **H**) and FTH (**G** and **I**) protein expression in ApoE$^{-/-}$ (n = 5) and WT (n = 3) mice; **J** and **K.** RT-PCR analysis of FTL (**J**) and FTH (**K**) mRNA expression in ApoE$^{-/-}$ (n = 4) and WT (n = 3) mice; **L-N.** Immunohistochemical examination of FTL protein expression in the cortex (**L**), hippocampus (**M**) and basal ganglia (**N**) of ApoE$^{-/-}$ (n = 4) and WT (n = 4) mice, Scale bar = 50 μm. Data were the mean ± SEM (% WT). *$p < 0.05$, **$p < 0.01$, ***$p < 0.001$ vs. WT mice.

regionally specific. The similarity patterns of FTL and FTH mRNA and protein expression implied that ApoE$^{-/-}$ affects their expression at the post-transcriptional level.

3.2. A region-specific effect of ApoE deficiency on expression of TfR1 and Fpn1 proteins in the brain

To explore how ApoE deficiency induced the regionally specific changes in brain iron contents, we measures the expression of TfR1 and Fpn1 proteins in the cortex, hippocampus and basal ganglia of ApoE$^{-/-}$ and WT mice at 1-, 2-, 4-, 10- and 24-months old. TfR1 and Fpn1 were examined because they are key controllers for the amount of iron import into (TfR1) and export from (Fpn1) cells [42,43]. Western blot analysis showed that TfR1 (Fig. 2A and B) and Fpn1 (Fig. 2A and C) expression in the cortex of ApoE$^{-/-}$ mice was not different from that in WT mice at all time-points. In the hippocampus, TfR1 expression (Fig. 2F and G) at 24-months was significantly higher and Fpn1 (Fig. 2F and H) at 2-, 4, 10- and 24 months lower in ApoE$^{-/-}$ than those in WT mice, while in the basal ganglia, TfR1 expression (Fig. 2K and L) at 2-, 4, 10- and 24-months was significantly higher and Fpn1 (Fig. 2K and M) at 2-, 4-, 10-months lower in ApoE$^{-/-}$ than those in WT mice. The findings collectively indicated that the progressive increase in iron contents in the hippocampus may be mainly due to the reduced Fpn1 expression, while that in the basal ganglia due to not only the reduced Fpn1 but also the elevated TfR1 expression. These findings revealed the existence of a region-specific effect of ApoE deficiency on expression of TfR1 and Fpn1 proteins, which may be one of the causes for the regionally specific changes in brain iron content in ApoE$^{-/-}$ mice.

3.3. Effects of ApoE deficiency on expression of IRPs and hepcidin were also regionally specific in the brain

Next, we answered the question of how ApoE deficiency led to the region-specific effect of on TfR1 and Fpn1 expression by investigating the effects of ApoE$^{-/-}$ on expression of IRPs and hepcidin in the in the cortex, hippocampus and basal ganglia of ApoE$^{-/-}$ and WT mice at 1-, 2-, 4-, 10- and 24-months old. IRPs and hepcidin expression was investigated because they are key controllers in TfR1 and Fpn1 expression at systemic and cellular levels; respectively [44,45]. It was found that in the cortex, there were no differences in expression of IRP1 (Fig. 2A and D) and IRP2 (Fig. 2A and E) between ApoE$^{-/-}$ and WT mice. In the hippocampus, the expression of IRP1 (Fig. 2F and I) and IRP2 (Fig. 2F

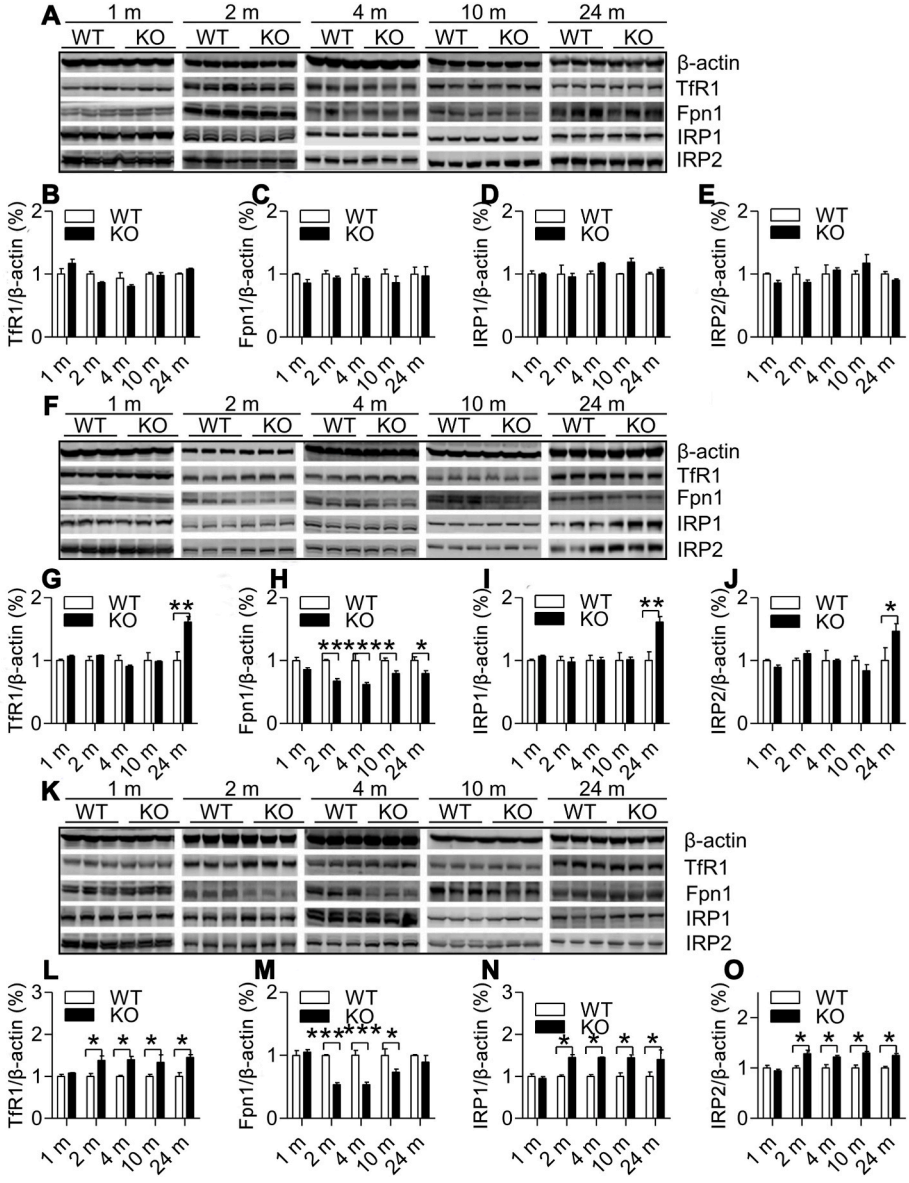

Fig. 2. Effects of ApoE deficiency on expression of TfR1, Fpn1, IRP1 and IRP2 in the cortex, hippocampus and basal ganglia of mice at 1-, 2-, 4-, 10- and 24-months old. Western blot analysis of expression of TfR1 (**A, B, F, G, K** and **L**), Fpn1 (**A, C, F, H, K** and **M**), IRP1 (**A, D, F, I, K** and **N**) and IRP2 (**A, E, F, J, K** and **O**) in the cortex (**A–E**), hippocampus (**F–J**) and basal ganglia (**K–O**) of ApoE$^{-/-}$ (n = 3) and WT (n = 3) mice at 1-, 2-, 4-, 10- and 24-months old. Data were the mean ± SEM (% WT). *p < 0.05, **p < 0.01,***p < 0.001 vs. WT mice.

and J) both at 24-months old were significantly higher in ApoE$^{-/-}$ than in WT mice. In the basal ganglia, the expression of IRP1 (Fig. 2K and N) and IRP2 (Fig. 2K and O) both at 2-, 4-, 10- and 24-months old were significantly higher in ApoE$^{-/-}$ than in WT mice. Also, ApoE$^{-/-}$ had no effect on hepcidin mRNA expression in the cortex (Fig. 3A). However, it induced a significant decline in expression of this peptide mRNA in the hippocampus (Fig. 3B) at 2-, 4-, 10- and 24-months old and in the basal ganglia (Fig. 3C) at 4-, 10- and 24-months old. The above findings showed that effects of ApoE$^{-/-}$ on expression of IRPs and hepcidin were also regionally specific in the brain and indicated that the up-regulated expression of IRPs may play an important causative role in ApoE$^{-/-}$-induced increase in TfR1 and reduction in Fpn1 expression in the hippocampus and basal ganglia.

3.4. ApoE deficiency induced a significant increase in HO-1 expression in different brain regions of mice aged 24 months old

To find out more about how ApoE deficiency induced an increase in brain iron contents, we also investigated the effects of ApoE deficiency on HO-1 expression in different brain regions of mice aged 24 months old because of the HO-1 is a rate-limiting enzyme in the catabolism of heme into ferrous iron, carbon monoxide, biliverdin [46] andHO1 activity is critical contribution to iron homeostasis.Western blot and RT-PCR analysis displayed that the expression of HO-1 protein (Fig. 3D and E) and mRNA (Fig. 3F) increased in all three brain regions including cortex, hippocampus and basal ganglia of ApoE$^{-/-}$ mice. The above results were further confirmed by immunofluorescence examination of HO-1 protein in different brain regions (Fig. 3G: Cortex; Fig. 3H: Hippocampus; Fig. 3I: Basal ganglia) of mice aged 24-months.

3.5. Effects of ApoE deficiency on expression of Aβ42 and MAP2 in different brain regions of mice aged 24 months old

The abnormal increase in brain iron has been associated with a number of neurodegenerative disorders including AD [10,43]. We therefore investigated effects of ApoE$^{-/-}$ and the increased iron on expression of a pathological marker of AD, Aβ42 and also MAP2 in the cortex, hippocampus and basal ganglia of mice at 24-months old. Western blot analysis demonstrated that Aβ42 expression (Fig. 4A and B) increased and MAP2 (Fig. 4A and C) decreased in three brain regions of ApoE$^{-/-}$ mice as compared with WT mice. The significant differences were found in the hippocampus and basal ganglia, but not in the cortex. Immunohistochemical examination manifested that expression of MAP2 (Fig. 4D) was also lower and Aβ42 (Fig. 4E) protein higher in the brain in ApoE$^{-/-}$ than in WT mice. In consistent with the reduced MAP2 and increased Aβ42 and iron contents, the number of TUNEL positive (apoptotic) neurons in the cortex (Fig. 4F), hippocampus (Fig. 4G) and basal ganglia (Fig. 4H) was higher in ApoE$^{-/-}$ than in WT mice, significant differences being found in the hippocampus (Fig. 4G) and basal ganglia (Fig. 4H) only.

3.6. Effects of ApoE deficiency on cytosolic aconitase activity in the cortex, hippocampus and basal ganglia of ApoE$^{-/-}$ and WT mice at 24-months old

We also measured cytoplasmic aconitase activity in the cortex, hippocampus, and basal ganglia. This is because IPR1 can act as either a cytoplasmic aconitase or an IRE (iron responsive element) binding protein, or cytoplasmic aconitase is a two-faced protein: the enzyme and IRP1 [47–49]. IRP1 is a [Fe–S] protein. IRP1 binding to IRE of both mRNAs of TfR1 and ferritin is regulated in response to the status of the iron sulfur cluster located near the center of IRP1 [50–52]. In iron-abundant cells, IRP1 contains a cubane 4Fe–4S cluster that prevents

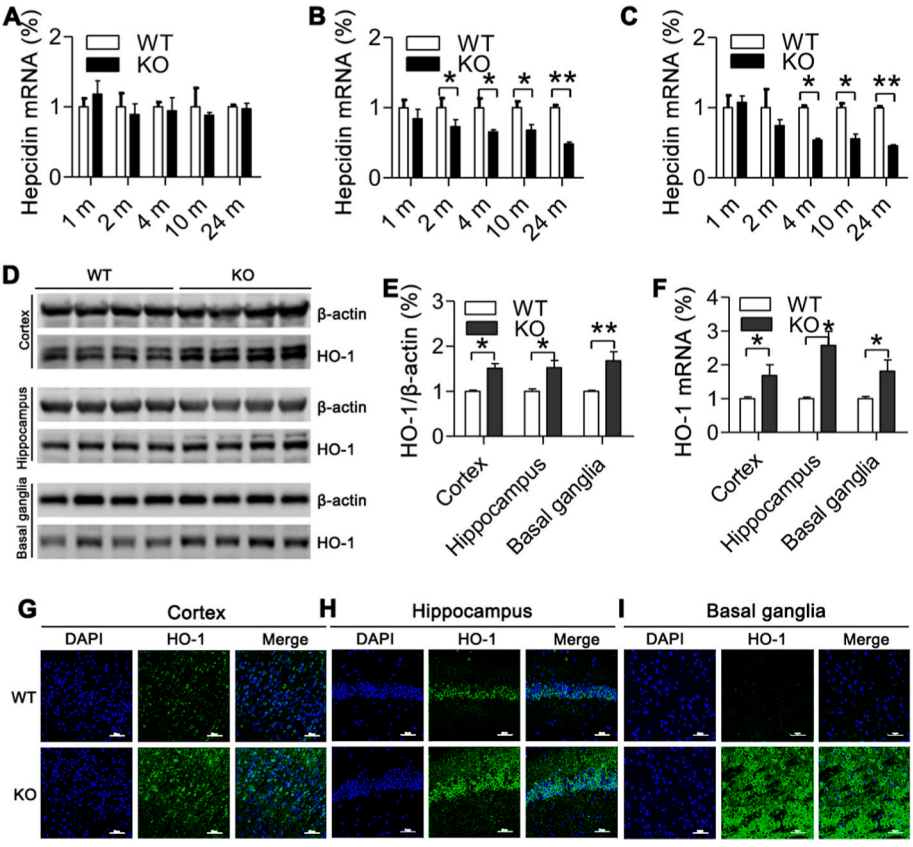

Fig. 3. Effects of ApoE deficiency on expression of hepcidin mRNA and HO-1 protein and mRNA in the cortex, hippocampus and basal ganglia of mice at 24-months old.
A-C. RT-PCR analysis of hepcidin mRNA expression of in the cortex (**A**), hippocampus (**B**) and basal ganglia (**C**) of ApoE$^{-/-}$ and WT mice at 24-months old; **D-F.** Western blot and RT-PCR analysis of HO-1 protein (**D** and **E**) and mRNA (**F**) expression in the cortex, hippocampus and basal ganglia of ApoE$^{-/-}$ and WT mice at 24-months old; **G-I.** Immunofluorescence examination of HO-1 protein expression in cortex (**G**), hippocampus (**H**) and basal ganglia (**I**) of ApoE$^{-/-}$ and WT mice at 24-months old (Scale bar = 50 μm). ApoE$^{-/-}$: n = 4; WT: n = 3. Data were the mean ± SEM (% WT). *p < 0.05, **p < 0.01, ***p < 0.001 vs. WT mice.

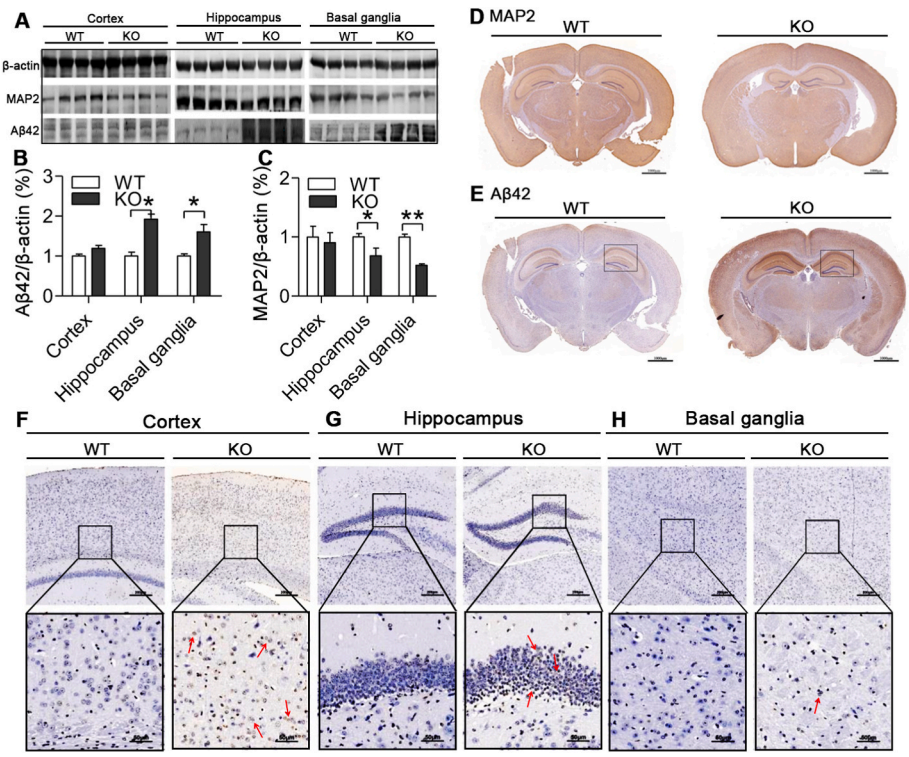

Fig. 4. Effects of ApoE deficiency on expression of Aβ42 and MAP2 protein and TUNEL positive neurons in the cortex, hippocampus and basal ganglia of mice at 24-months old.
A-C. Western blot analysis of Aβ42 (**A** and **B**) and MAP2 (**A** and **C**) protein expression in the cortex, hippocampus and basal ganglia of ApoE$^{-/-}$ (n = 4) and WT (n = 4) mice at 24-months; **D** and **E**. Immunohistochemical examination of MAP2 (**D**) and Aβ42 (**E**) protein expression in the brain (Scale bar = 1000 μm) of ApoE$^{-/-}$ and WT mice at 24-months old; **F–H**. Tunel staining in the cortex (**F**), hippocampus (**G**) and basal ganglia (**H**) (10X, Scale bar = 200 μm; 40X, Scale bar = 50 μm) of ApoE$^{-/-}$ and WT mice at 24-months old. Data were the mean ± SEM (% WT). *p < 0.05, **p < 0.01, ***p < 0.001 vs. WT mice.

IRE binding and displays aconitase activity. In iron-poor cells, such a Fe–S cluster does not exist and IRP1 functions as an IRE binding protein [52]. In short, the changes in cytoplasmic aconitase activity may reflect the binding activity of IRP1.

In contrast to the ApoE KO-induced increase of IRP1 expression, cytosolic aconitase activity was found to be significantly lower in hippocampus (Supplementary Fig. 2B) and basal ganglia (Supplementary Fig. 2C) of ApoE$^{-/-}$ mice than in those of WT mice at 24-months old. There was no significant difference in the activity of aconitase in the cortex of ApoE$^{-/-}$ and WT mice (Supplementary Fig. 2A), which was consistent with the effect of ApoE KO on the expression of IRP1 in this brain region. This study provides further evidence for the positive role of ApoE$^{-/-}$ in IRP1 expression.

3.7. Effects of ApoE deficiency on the contents of MDA and 8-isoprostane and the expression of Gpx4 and cytokines in different brain regions of mice aged 24 months old

We therefore investigated effects of ApoE$^{-/-}$ and the increased iron on the indexes of reactive oxygen species (ROS), MDA and 8-isoprostane, Gpx4 (a key inhibitor of ferroptosis) and inflammatory cytokines, TNFα, IL-1β and IL-6 as well as anti-inflammatory cytokine IL-10 in the cortex, hippocampus and basal ganglia of mice at 24-months old. The findings showed that the contents of MDA (Fig. 5A) were significantly increased in thecortex, hippocampus, basal ganglia and 8-isoprostane (Fig. 5B) in the hippocampus and basal ganglia of ApoE$^{-/-}$ mice as compared with WT mice. RT-PCR demonstrated that ApoE$^{-/-}$ had no effect on anti-inflammatory cytokine IL-10 (Fig. 5C) in three brain regions, but significantly increased IL-1β (Fig. 5D) and IL-6 (Fig. 5E) in the hippocampus and basal ganglia and up-regulated TNFα (Fig. 5F) mRNA and down-regulated Gpx4 mRNA (Fig. 5G) expression in the cortex, hippocampus and basal ganglia of mice at 20-months old.

3.8. Replenishment of ApoE partially reversed the iron-related phenotype in ApoE$^{-/-}$ mice

Finally, we examined the effects of ApoE over-expression on iron content, ApoE, FTL protein, 8-isoprostane, IL-6, IL-10 and Gpx4 expression in the brain of ApoE$^{-/-}$ mice at 24-months old. ApoE$^{-/-}$ mice were treated with 2 μL of Ad-ApoE or Ad-blank by intracerebroventricular (ICV) injection, and 7 days later the relevant measurements were performed. The expression of ApoE in the basal ganglia (Fig. 5I) was found to be significantly increased, simultaneously, the iron contents (Fig. 5H) and expression of FTL protein (Fig. 5J and K) in the hippocampus (Fig. 5J) and basal ganglia (Fig. 5K) decreased in ApoE$^{-/-}$ mice treated with Ad-ApoE as compared with those treated with Ad-blank. In addition, the expression of the ROS index 8-isoprostane (Fig. 5L) and the inflammatory cytokine IL-6 (Fig. 5N) was significantly lower and the key inhibitor of ferroptosis Gpx4 (Fig. 5O) higher in the basal ganglia of ApoE−/− mice treated with Ad-ApoE than that of ApoE−/− mice treated with Ad-blank. The treatment with Ad-ApoE did not induce any overt changes in the expression of anti-inflammatory cytokine IL-10 in the basal ganglia of ApoE−/− mice (Fig. 5M). The data demonstrated that Ad-ApoE could increase ApoE expression and then counteract the increase of iron in the hippocampus and basal ganglia under ApoE−/− condition, reducing the concomitant ROS, inflammation, and ferroptosis level and partially reversing the iron-related phenotype induced by ApoE deficiency.

4. Discussion

The major objective of the present study was to find out whether ApoE can affect brain iron homeostasis as it works outside brain. By measuring total iron contents and FTL and FTH expression in ApoE$^{-/-}$ and WT mice at different ages, we demonstrated that the complete absence of ApoE can lead to a significant increase in iron contents and FTL and FTH expression in the hippocampus and basal ganglia, but not in the cortex of the brain in mice at 10- and/or 24 months old. Treatment with Ad-ApoE significantly increased ApoE protein and Gpx4 expression

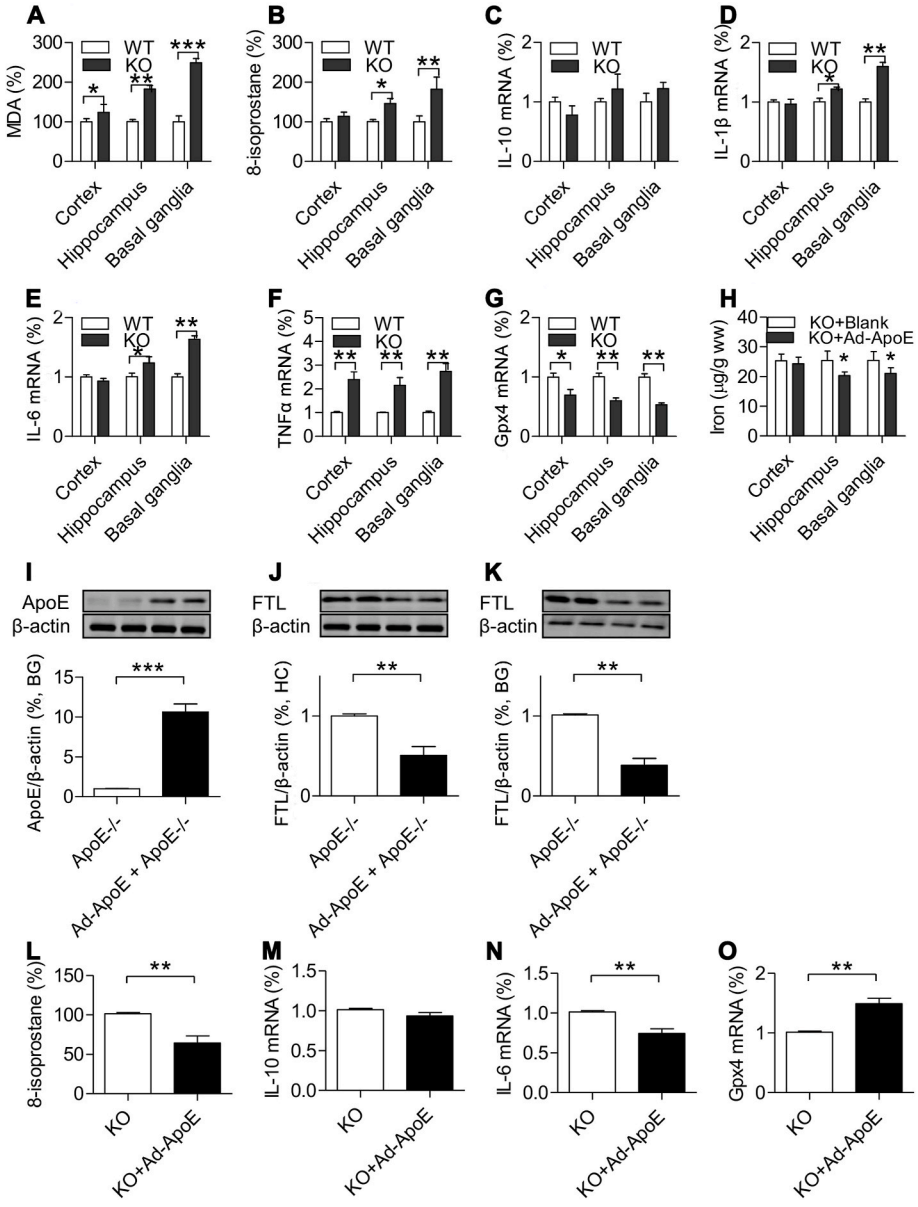

Fig. 5. A–G: Effects of ApoE deficiency on the contents of malondialdehyde (MDA) and 8-isoprostane and the expression of IL-10, IL1β, IL-6, TNFα and Gpx-4 mRNA in the cortex, hippocampus and basal ganglia mice at 24-months old (n = 4 in ApoE−/− and n = 3 in WT).
A. MDA was measured by the thiobarbituric acid (TBA) reaction with a commercial kit; **B.** 8-isoprostane was determined using an ELISA Kit; **C-G.** RT-PCR analysis of IL-10 (**C**), IL1β (**D**), IL-6 (**E**), TNFα (**F**) and Gpx-4 (**G**) mRNA expression of in the cortex, hippocampus and basal ganglia of ApoE$^{-/-}$ and WT mice at age of 24-months old; **H–O**. Replenishment of ApoE partially reversed the iron-related phenotype in ApoE$^{-/-}$ mice. ApoE$^{-/-}$ mice at 24-months old were treated with 2 μL of Ad-ApoE or Ad-blank by intracerebroventricular (ICV) injection, and 7 days later the relevant measurements were performed (n = 4 in ApoE−/− + Ad-ApoE, and n = 3 in ApoE−/− + Ad-blank). **H**. Iron contents in the cortex, hippocampus and basal ganglia of Ad-ApoE or Ad-blank treated ApoE−/− mice at 24-months old. **I–K**. Western blot analysis of ApoE expression in basal ganglia (**I**) and FTL expression in the hippocampus (**J**) and basal ganglia (**K**) of Ad-ApoE or Ad-blank treated ApoE−/− mice at 24-months old. **L**. 8-isoprostane was measured using a ELISA Kit; and **M-O**: RT-PCR analysis of IL-10 (**M**), IL-6 (**O**) and Gpx-4 (**P**) mRNA expression in the basal ganglia of Ad-ApoE or Ad-blank treated ApoE−/− mice at 24-months old. Data are the mean ± SEM (A–G: % WT; H–O: % KO). *p < 0.05, **p < 0.01, ***p < 0.001 vs. WT mice or Ad-blank treated ApoE−/− mice.

as well as reduced iron content, and FTL expression, ROS (8-isoprostan) and the inflammatory cytokine (IL-6) levels in these two brain regions in mice at 24 months old, indicating that replenishment of the absent ApoE can reduce the concomitant ROS, inflammation, and ferroptosis levels and partly reverse the iron-related phenotype in ApoE$^{-/-}$ mice by increasing ApoE expression. These results showed for the first time that ApoE might be required for iron homeostasis in the brain.

To find out why iron contents increased in the hippocampus and basal ganglia in ApoE$^{-/-}$ mice, we next investigated TfR1 and Fpn1 expression because iron levels in most types of cells depend on the expression of these two transporters [7,53]. We found that the expression of TfR1 is significantly higher and Fpn1 lower in the hippocampus and basal ganglia of brain in ApoE$^{-/-}$ mice than that in WT mice, while in the cortex, the expression of these two iron-transporters in ApoE$^{-/-}$ mice does not differ from that in WT mice. These results indicated that the increased iron contents are mainly due to the enhanced cell-iron import by up-regulated TfR1 and the reduced cell-iron export by down-regulated Fpn1 (Fig. 6). In addition, the increased expression of HO-1 induced by ApoE deficiency might be partly associated with the rise of free iron in these brain regions of mice.

Studies have demonstrated that expression TfR1 and Fpn1 is controlled by not only IRPs but also hepcidin. In the present study, we demonstrated that ApoE$^{-/-}$ induced a significant increase in expression of IRP1 and IRP2 in the hippocampus (24-months) and basal ganglia (2-, 4-, 10- and 24-months) as well as a significant decrease of cytosolic aconitase activity in the hippocampus (24-months) and the basal ganglia (24-months), but not in the cortex of the brain in mice. The increased IRP1 and IRP2 expression could lead to an increase in the binding of IRPs to cognate IREs in the 3'-untranslated regions of TfR1 and in the 5'-untranslated regions of Fpn1 mRNAs, and then promoted TfR1 mRNA translation and stabilizing TfR1 mRNA against endonucleolytic degradation as well as inhibited Fpn1 mRNA translation, ultimately, resulting in a significant increase in TfR1 and reduction in Fpn1 expression [54,55]. The expression of TfR1 and Fpn1 is also regulated systemically by hepcidin [44,45,56,57]. Fpn1 is the membrane receptor of hepcidin and the binding of hepcidin with Fpn1 induces the internalization and degradation of the hepcidin/Fpn1 complex, reducing fpn1 and thus suppressing the export of iron from the cells [58–60]. The increased hepcidin could lead to a reduction in Fpn1. In the present study, however, hepcidin was found to be down-regulated, rather than

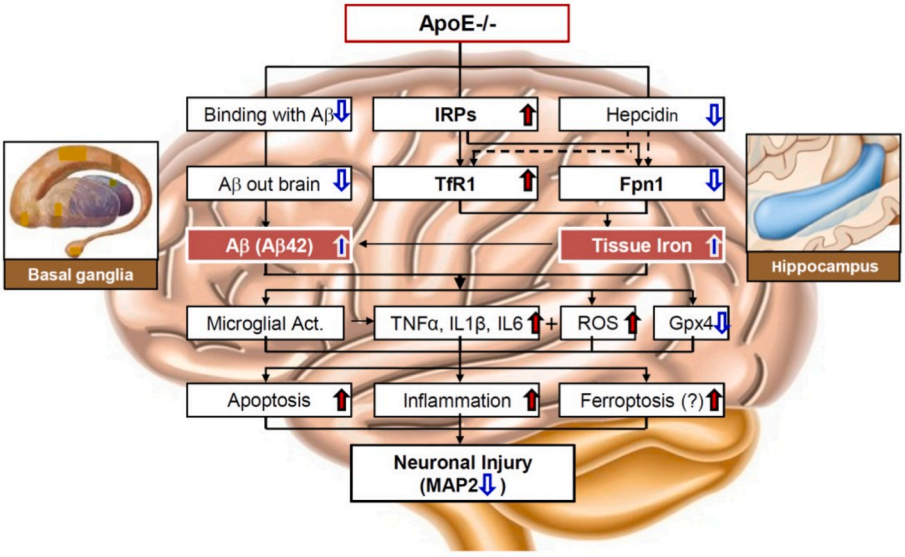

Fig. 6. A hypothetical scheme for the increased iron in the hippocampus and basal ganglia of in apolipoprotein E knock-out mice. The increased iron in the hippocampus and basal ganglia of ApoE−/− mice might be due to the increased expression of IRPs (iron regulatory proteins, IRP1 and IRPs) which unregulates TfR1 expression and TfR1 mediated cell-iron import as well as down-regulates Fpn1 expression and Fpn1-mediated cell-iron export. ApoE knock-out induces a reduction in hepcidin expression, removing the inhibition of hepcidin on TfR1 expression, which may be also partly associated with up-regulation of TfR1. ApoE deficiency reduces the binding activities of ApoE with Aβ and then the elimination of toxic Aβ peptides out of the brain, leading to a increased toxic Aβ peptides (Aβ42). ApoE deficiency induces neuronal injury, as reflected by the reduced neuron MAP2 (microtubule-associated protein 2) and the increased number of TUNEL positive (apoptotic) neurons, may be mainly caused by the increased iron and accumulation of toxic Aβ peptides and subsequently microglial activation, inflammation and oxidative stress, apoptosis and may be also ferroptosis as demonstrated by the increased inflammatory cytokines IL-1β (Interleukin-1β), IL-6 (Interleukin-6), TNFα (Tumor necrosis factor-α), ROS (reactive oxygen species), MDA (malondialdehyde) and 8-isoprostane and the reduced Gpx4 (glutathione peroxidase 4).

up-regulated in hippocampus and basal ganglia of ApoE$^{-/-}$ mice. The reduced expression of hepcidin might be due to the ApoE$^{-/-}$-induced increase in iron contents in these two brain regions. Take together, the above results revealed that the increased TfR1 and decreased Fpn1 in the hippocampus and basal ganglia were mainly caused by the ApoE$^{-/-}$-induce upregulation of IRPs induced by ApoE deficiency rather than hepcidin. The reduced hepcidin may partly play a role in the up-regulation of TfR1 in the hippocampus and basal ganglia of ApoE$^{-/-}$ mice (Fig. 6) because hepcidin has been demonstrated to have an inhibiting role on TfR1 expression in different types of cells [61–63].

ApoE has been reported to be able to bind with Aβ and then eliminate toxic Aβ peptides out of the brain via ApoE receptors [11]. The increased Aβ42 found in the hippocampus and basal ganglia of ApoE$^{-/-}$ mice at 24-months old indicated that ApoE deficiency could lead to an increase in accumulation of toxic Aβ peptides in the brain, probably by reducing the binding activities of ApoE with Aβ and the amount of toxic Aβ peptides out of the brain. The findings support the notion that ApoE may contribute to AD pathogenesis. In addition to the increased toxic Aβ peptides, neuronal injury induced by ApoE$^{-/-}$, as reflected by the reduced MAP2 and the increased number of TUNEL positive (apoptotic) neurons, may be also associated with the increased iron and iron-induced ROS, as demonstrated by the increased MDA and 8-isoprostane in the hippocampus and basal ganglia of ApoE$^{-/-}$ mice at 24-months old [11,17].

Moreover, the activated microglia may also contribute to neuronal injury because microglia, once activated, are thought to release a variety of inflammatory and cytotoxic mediators such as TNF-α, IL-1β, IL-6 and also ROS [64]. The increased TNF-α, IL-1β, IL-6 and ROS found in the hippocampus and basal ganglia of ApoE$^{-/-}$ mice supported this viewpoint. Ferroptosis is a recently recognized form of regulated cell death which is characterized by the accumulation of lipid peroxidation products and generation of lethal ROS, particularly lipid hydroperoxides derived from iron metabolism [65,66] and Gpx4, an antioxidant defense enzyme capable of repairing lipid oxidative damage, is a key inhibitor of ferroptosis [67,68]. Therefore, the significant reduced Gpx4 implied that ferroptosis may also play a role in ApoE$^{-/-}$-induced neuronal injury. Further work is clearly required to substantiate this possibility.

ApoE has been shown to have antioxidant activity in cell culture and is associated with antioxidative activity in vivo [69–71]. Conditioned medium from ApoE-transfected macrophage cell culture protects neuronal cell culture against oxidative environments, such as hydrogen peroxide. Mice lacking apoE have increased markers of oxidative damage in both the cardiovascular system and the brain [69,70,72]. Although the arginine- and lysine-rich region between residues 140 and 160 in the N-terminal domain of apoE has been found to be necessary and sufficient for antioxidant activity [73], the relevant mechanisms involved in the antioxidant activity of ApoE remain largely undefined. Accumulated data showed that a progressive accumulation of iron with age in atherosclerotic lesions and tissue sections of the heart [74], liver, spleen and aortic tissues [21,22] and also in the brain as we found in the present study in ApoE deficient mice. These might suggest that ApoE has an inhibitory effect on iron contents in the cells or tissues under physiological conditions, which might be one of mechanisms involved in the antioxidant activity of ApoE. Further studies about these possibilities are needed.

The significant increase in iron contents and ferritin expression was found in the hippocampus and basal ganglia but not in the cortex in ApoE$^{-/-}$ mice, indicating a regionally specific effect of ApoE deficiency on brain iron status. In consistent with the findings about iron contents and ferritin expression, the effects of ApoE$^{-/-}$ on the expression of TfR1, Fpn1, IRPs and hepcidin are also regionally specific, the significant effects being also found in the in the hippocampus and basal ganglia but not in the cortex. In addition, the significant increase in the levels of Aβ42, MAP2, 8-isoprostane, IL-1β, and IL-6 was also found in the hippocampus and basal ganglia but not in the cortex. Although the significant increase in the contents of MDA, Gpx4 TNF-α was found in all three brain regions we examined, the difference ($P < 0.05$) in the cortex is much smaller than that ($P < 0.01$) in the hippocampus and basal ganglia. The regionally effects of ApoE$^{-/-}$ may be due to the uneven distribution of iron and the relevant metabolic proteins in the brain [75]. The basal ganglia contains the highest level of iron [76]. This may be a major reason of why the significant changes in iron content were found in this brain region of ApoE$^{-/-}$ mice. In addition, our recent study showed that Apo$^{-/-}$ has no effects on expression of IRPs in peripheral organs [21]. However, in the current study, we found that ApoE$^{-/-}$ upregulates expression of IRPs in some brain regions. These suggest that the effect of ApoE on expression of IRPs is not only regionally but also organ-specific. The relevant mechanisms are unknown and further investigations are needed.

5. Conclusion

In summary, we showed that ApoE deficiency can significantly increase iron contents in the hippocampus and basal ganglia, but not in the cortex of the brain at aged mice by up-regulating TfR1 expression and TfR1 mediated cell-iron import as well as down-regulating Fpn1 expression and Fpn1-mediated cell-iron export, mainly via the up-regulation of IRPs. We also demonstrated that replenishment of the absent ApoE can partly reverse the iron-related phenotype in ApoE$^{-/-}$ mice. These findings collectively indicated that ApoE may be required for physiological iron homeostasis in the brain. In addition, the findings revealed that neuronal injury induced by ApoE deficiency may be mainly resulted from the increased iron and accumulation of toxic Aβ peptides and subsequently microglial activation, inflammation and oxidative stress, apoptosis and may be also ferroptosis. Our findings provided a piece of novel evidence that iron is a key link between ApoE and AD development and also imply that ApoE deficiency and reduced ApoE expression could be one of the causes for the unexplained increase in brain iron in some neurodegenerative patients.

Authors' contributions

J.M., M.Q.S., W.L., and Q.Z. carried out the animal- and cell-experiments and collected data; J.M. and Q.G contributed to the analysis of data and generated figures; Q.G. wrote and revised the manuscript. Z.M.Q. designed and supervised the study, analyzed the data and contributed to the writing of the manuscript.

Funding

The studies in our laboratories were supported by the National Natural Science Foundation of China (NSFC82003702-Q.G., NSFC31571195-Z.M.Q.) and Public Welfare Scientifc Research Project of Futian District Shenzhen (FTWS2019024-Q.Z.)

Ethics approval and consent to participate

The study was approved by the Institutional Animal Care and Use Committee of Nantong University in Nantong, China.

Availability of supporting data

All data generated or analyzed during this study are included either in this article or in the supplementary information files.

Declaration of competing interest

No conflict of interest.

Acknowledgements

We would like to thank Christopher Qian from The Chinese University of Hong Kong for assisting with the preparation and English revision of the manuscript.

Appendix A. Supplementary data

Supplementary data to this article can be found online at https://doi.org/10.1016/j.redox.2023.102779.

References

[1] A. Ashraf, M. Clark, P.W. So, The aging of iron man, Front. Aging Neurosci. 10 (2018) 65.
[2] S. Ayton, P. Lei, A.I. Bush, Metallostasis in Alzheimer's disease, Free Radic. Biol. Med. 62 (2013) 76–89.
[3] S. Ayton, et al., Cerebral quantitative susceptibility mapping predicts amyloid-beta-related cognitive decline, Brain 140 (2017) 2112–2119.
[4] A.A. Belaidi, A.I. Bush, Iron neurochemistry in Alzheimer's disease and Parkinson's disease: targets for therapeutics, J. Neurochem. 139 (2016) 179–197.
[5] S. van Duijn, et al., Cortical iron reflects severity of alzheimer's disease, J. Alzheimers Dis. 60 (2017) 1533–1545.
[6] A. Pal, et al., Iron in alzheimer's disease: from physiology to disease disabilities, Biomolecules 12 (2022) 1248.
[7] Z.M. Qian, Q. Wang, Expression of iron transport proteins and excessive iron accumulation in the brain in neurodegenerative disorders, Brain Res. Rev. 27 (1998) 257–267.
[8] S.A. Kent, et al., The physiological roles of tau and Aβ: implications for Alzheimer's disease pathology and therapeutics, Acta Neuropathol. 140 (2020) 417–447.
[9] T.A. Rouault, Iron on the brain, Nat. Genet. 28 (2001) 299–300.
[10] Y. Ke, Z. Ming Qian, Iron misregulation in the brain: a primary cause of neurodegenerative disorders, Lancet Neurol. 2 (2003) 246–253.
[11] P.B. Verghese, et al., ApoE influences amyloid-β (Aβ) clearance despite minimal apoE/Aβ association in physiological conditions, Proc. Natl. Acad. Sci. USA 110 (2013) E1807–E1816.
[12] K. Greenow, N.J. Pearce, D.P. Ramji, The key role of apolipoprotein E in atherosclerosis, J. Mol. Med. (Berl.) 83 (2005) 329–342.
[13] K.L. Rasmussen, Plasma levels of apolipoprotein E, APOE genotype and risk of dementia and ischemic heart disease: a review, Atherosclerosis 255 (2016) 145–155.
[14] V.B. Gupta, et al., Plasma apolipoprotein E and Alzheimer disease risk: the AIBL study of aging, Neurology 76 (2011) 1091–1098.
[15] S.H. Han, et al., Both targeted mass spectrometry and flow sorting analysis methods detected the decreased serum apolipoprotein E level in Alzheimer's disease patients, Mol. Cell. Proteomics 13 (2014) 407–419.
[16] S. Ayton, et al., Ferritin levels in the cerebrospinal fluid predict Alzheimer's disease outcomes and are regulated by APOE, Nat. Commun. 6 (2015) 6760.
[17] Y. Uchida, et al., APOE ϵ4 dose associates with increased brain iron and β-amyloid via blood-brain barrier dysfunction, J. Neurol. Neurosurg. Psychiatry jnnp (2022) 2021–328519.
[18] Y. Zhang, et al., Current understanding of the interactions between metal ions and Apolipoprotein E in Alzheimer's disease, Neurobiol. Dis. 172 (2022), 105824.
[19] L. Mahoney-Sanchez, et al., The complex role of apolipoprotein E in Alzheimer's Disease: an overview and update, J. Mol. Neurosci. 60 (2016) 325–335.
[20] H. Wood, Alzheimer disease: iron–the missing link between ApoE and Alzheimer disease? Nat. Rev. Neurol. 11 (2015) 369.
[21] J. Ma, et al., Apolipoprotein E deficiency induces a progressive increase in tissue iron contents with age in mice, Redox Biol. 40 (2021), 101865.
[22] J. Ma, et al., The role of iron in atherosclerosis in apolipoprotein E deficient mice, Front. Cardiovasc. Med. 9 (2022), 857933.
[23] Y.F. Zhou, et al., Cystathionine β-synthase is required for body iron homeostasis, Hepatology 67 (2018) 21–35.
[24] Z.M. Qian, et al., Increased nitric oxide is one of the causes of changes of iron metabolism in strenuously exercised rats, Am. J. Physiol. 280 (2001) R739–R743.
[25] L.N. Lu, et al., Expression of iron transporters and pathological hallmarks of Parkinson's and Alzheimer's Diseases in the brain of young, adult, and aged rats, Mol. Neurobiol. 54 (2017) 5213–5224.
[26] F.L. Zhang, et al., Impairment of hepcidin upregulation by lipopolysaccharide in the interleukin-6 knockout mouse brain, Front. Mol. Neurosci. 10 (2017) 367.
[27] Z.M. Qian, et al., Expression of ferroportin1, hephaestin and ceruloplasmin in rat heart, Biochim. Biophys. Acta 1772 (2007) 527–532.
[28] F. Du, et al., Hyperthermic preconditioning protects astrocytes from ischemia/reperfusion injury by up-regulation of HIF-1 alpha expression and binding activity, Biochim. Biophys. Acta 1802 (2010) 1048–1053.
[29] W. He, et al., Ginkgolides mimic the effects of hypoxic preconditioning to protect C6 cells against ischemic injury by up-regulation of hypoxia-inducible factor-1 alpha and erythropoietin, Int. J. Biochem. Cell Biol. 40 (2008) 651–662.
[30] Z.M. Qian, et al., Lipopolysaccharides upregulate hepcidin in neuron via microglia and the IL-6/STAT3 signaling pathway, Mol. Neurobiol. 50 (2014) 811–820.
[31] Z.M. Qian, et al., Development and iron-dependent expression of hephaestin in different brain regions of rats, J. Cell. Biochem. 102 (2007) 1225–1233.
[32] K.P. Ho, et al., Exercise decreases cytosolic aconitase activity in the liver, spleen, and bone marrow in rats, Biochem. Biophys. Res. Commun. 282 (2001) 264–267.
[33] Y. Ke, et al., Age-dependent and iron-independent expression of two mRNA isoforms of divalent metal transporter 1 in rat brain, Neurobiol. Aging 26 (2005) 739–748.
[34] Y.Z. Chang, et al., Increased divalent metal transporter 1 expression might be associated with the neurotoxicity of L-DOPA, Mol. Pharmacol. 69 (2006) 968–974.
[35] S.T. Zhao, X.T. Huang, C. Zhang, Y. Ke, Humanin protects cortical neurons from ischemia and reperfusion injury by the increased activity of superoxide dismutase, Neurochem. Res. 37 (2012) 153–160.
[36] J. Gong, et al., Pre-treatment of rats with ad-hepcidin prevents iron-induced oxidative stress in the brain, Free Radic. Biol. Med. 90 (2016) 126–132.
[37] G. Yang, et al., Hepcidin attenuates the iron-mediated secondary neuronal injury after intracerebral hemorrhage in rats, Transl. Res. S1931–5244 (2020), 30224-3.
[38] L. Zhao, et al., Amyloid beta-peptide 31-35-induced neuronal apoptosis is mediated by caspase-dependent pathways via cAMP-dependent protein kinase A activation, Aging Cell 7 (2008) 47–57.
[39] F. Du, et al., Purity, cell viability, expression of GFAP and bystin in astrocytes cultured by different procedures, J. Cell. Biochem. 109 (2010) 30–37.

[40] Y. Liu, et al., CX3CL1/CX3CR1-mediated microglia activation plays a detrimental role in ischemic mice brain via p38MAPK/PKC pathway, J. Cerebr. Blood Flow Metabol. 35 (2015) 1623–1631.
[41] L. Zhu, et al., Correlation between the expression of divalent metal transporter 1 and the content of hypoxia-inducible factor-1 in hypoxic HepG2 cells, J. Cell Mol. Med. 12 (2008) 569–579.
[42] M.W. Hentze, M.U. Muckenthaler, N.C. Andrews, Balancing acts: molecular control of mammalian iron metabolism, Cell 117 (2004) 285–297.
[43] Y. Ke, Z.M. Qian, Brain iron metabolism: neurobiology and neurochemistry, Prog. Neurobiol. 83 (2007) 149–173.
[44] B. Galy, et al., Iron regulatory proteins are essential for intestinal function and control key iron absorption molecules in the duodenum, Cell Metabol. 7 (2008) 79–85.
[45] M.W. Hentze, M.U. Muckenthaler, B. Galy, C. Camaschella, Two to tango: regulation of Mammalian iron metabolism, Cell 142 (2010) 24–38.
[46] O. Pol, The role of carbon monoxide, heme oxygenase 1, and the Nrf2 transcription factor in the modulation of chronic pain and their interactions with opioids and cannabinoids, Med. Res. Rev. 41 (2021) 136–155.
[47] H. Beinert, M.C. Kennedy, Aconitase, a two-faced protein: enzyme and iron regulatory factor, Faseb. J. 7 (1993) 1442–1449.
[48] J. Narahari, R. Ma, M. Wang, W.E. Walden, The aconitase function of iron regulatory protein 1. Genetic studies in yeast implicate its role in iron-mediated redox regulation, J. Biol. Chem. 275 (2000) 16227–16234.
[49] J. Saas, K. Ziegelbauer, A. von Haeseler, B. Fast, M. Boshart, A developmentally regulated aconitase related to iron-regulatory protein-1 is localized in the cytoplasm and in the mitochondrion of Trypanosoma brucei, J. Biol. Chem. 275 (2000) 2745–2755.
[50] M.W. Hentze, P. Argos, Homology between IRE-BP, a regulatory RNA-binding protein, aconitase, and isopropylmalate isomerase, Nucleic Acids Res. 19 (1991) 1739–1740.
[51] D.J. Haile, T.A. Rouault, C.K. Tang, J. Chin, J.B. Harford, R.D. Klausner, Reciprocal control of RNA-binding and aconitase activity in the regulation of the iron-responsive element binding protein: role of the iron-sulfur cluster, Proc. Natl. Acad. Sci. U. S. A. 89 (1992) 7536–7540.
[52] G. Weiss, B. Goossen, W. Doppler, D. Fuchs, K. Pantopoulos, G. Werner-Felmayer, H. Wachter, M.W. Hentze, Translational regulation via iron-responsive elements by the nitric oxide/NO-synthase pathway, EMBO J. 12 (1993) 3651–3657.
[53] H. Drakesmith, E. Nemeth, T. Ganz, Ironing out ferroportin, Cell Metabol. 22 (2015) 777–787.
[54] M.D. Knutson, Iron-sensing proteins that regulate hepcidin and enteric iron absorption, Annu. Rev. Nutr. 30 (2010) 149–171.
[55] N. Wilkinson, K. Pantopoulos, The IRP/IRE system in vivo: insights from mouse models, Front. Pharmacol. 5 (2014) 176.
[56] Z.M. Qian, Y. Ke, Brain iron transport, Biol. Rev. 94 (2019) 1672–1684.
[57] Z.M. Qian, Y. Ke, Hepcidin and its therapeutic potential in neurodegenerative disorders, Med. Res. Rev. 40 (2020) 633–653.
[58] S. Abound, D.J. Haile, A novel mammalian iron-regulated protein involved in intracellular iron metabolism, J. Biol. Chem. 275 (2000) 19906–19912.
[59] A. Donovan, et al., Positional cloning of zebrafish ferroportin1 identifies a conserved vertebrate iron exporter, Nature 403 (2000) 776–781.
[60] A.T. McKie, et al., A novel duodenal iron-regulated transporter, IREG1, implicated in the basolateral transfer of iron to the circulation, Mol. Cell. 5 (2000) 299–309.
[61] M.U. Muckenthaler, B. Galy, M.W. Hentze, Systemic iron homeostasis and the iron-responsive element/iron-regulatory protein (IRE/IRP) regulatory network, Annu. Rev. Nutr. 28 (2008) 197–213.
[62] F. Du, et al., A synergistic role of hyperthermic and pharmacological preconditioning to protect astrocytes against ischemia/reperfusion injury, Neurochem. Res. 36 (2011) 312–318.
[63] F. Du, et al., Hepcidin suppresses brain iron accumulation by downregulating iron transport proteins in iron-overloaded rats, Mol. Neurobiol. 52 (2015) 101–114.
[64] Z.Z. Chong, F. Li, K. Maiese, Oxidative stress in the brain: novel cellular targets that govern survival during neurodegenerative disease, Prog. Neurobiol. 75 (2005) 207–246.
[65] S.J. Dixon, et al., Ferroptosis: an iron-dependent form of nonapoptotic cell death, Cell 149 (2012) 1060–1072.
[66] S.J. Dixon, B.R. Stockwell, The role of iron and reactive oxygen species in cell death, Nat. Chem. Biol. 10 (2014) 9–17.
[67] A.R. Bogdan, M. Miyazawa, K. Hashimoto, Y. Tsuji, Regulators of iron homeostasis: new players in metabolism, cell death, and disease, Trends Biochem. Sci. 41 (2016) 274–286.
[68] T. Zhao, et al., Regulating Nrf2-GPx4 axis by bicyclol can prevent ferroptosis in carbon tetrachloride-induced acute liver injury in mice, Cell Death Dis. 8 (2022) 380.
[69] K.S. Montine, et al., Distribution of reducible 4-hydroxynonenal adduct immunoreactivity in Alzheimer disease is associated with APOE genotype, J. Neuropathol. Exp. Neurol. 57 (1998) 415–425.
[70] J.N. Keller, et al., Amyloid beta-peptide effects on synaptosomes from apolipoprotein E-deficient mice, J. Neurochem. 74 (2000) 1579–1586.
[71] B.O. Botchway, et al., Alzheimer disease: recent updates on apolipoprotein E and gut microbiome mediation of oxidative stress, and prospective interventional agents, Aging Dis 13 (2022) 87–102.
[72] M. Miyata, J.D. Smith, Apolipoprotein E allele-specific antioxidant activity and effects on cytotoxicity by oxidative insults and beta-amyloid peptides, Nat. Genet. 14 (1996) 55–61.
[73] T. Pham, A. Kodvawala, D.Y. Hui, The receptor binding domain of apolipoprotein E is responsible for its antioxidant activity, Biochemistry 44 (2005) 7577–7582.
[74] T.S. Lee, et al., Iron-deficient diet reduces atherosclerotic lesions in apoE-deficient mice, Circulation 99 (1999) 1222–1229.
[75] Z. Qian, Q. Wang, Y. Pu, Brain iron and neurological disorders, Chin. Med. J. 110 (1997) 455–458.
[76] S.A. Benkovic, J.R. Connor, Ferritin, transferrin, and iron in selected regions of the adult and aged rat brain, J. Comp. Neurol. 338 (1993) 97–113.